New Phytologist

Research

Cryptic CAM photosynthesis in Joshua tree (*Yucca brevifolia*, *Y. jaegeriana*)

Karolina Heyduk[1,2], Sara Sciulla[3], Bridget Hennessy[4], Madeline Czymmek[4], Edward V. McAssey[1,2], Chase Kane[2], G Young Kim[1,2], Ifeoluwa Sogunle[1], Lulu Heublein[1], Dhriti Sriram[5], Bryan MacNeill[6], Michael T. Hren[7], Todd C. Esque[3], Jeremy B. Yoder[8], Michael R. McKain[6], Christopher Irwin Smith[5] and Lesley A. DeFalco[3]

[1]Department of Ecology and Evolutionary Biology, University of Connecticut, Storrs, CT 06269, USA; [2]School of Life Sciences, University of Hawai'i at Mānoa, Honolulu, HI 96822, USA; [3]U.S. Geological Survey, Western Ecological Research Center, Boulder City Field Station, Boulder City, NV 89005, USA; [4]Chicago Botanical Garden, Glencoe, IL 60022, USA; [5]Department of Biology, Willamette University, Salem, OR 97301, USA; [6]Department of Biological Sciences, University of Alabama, Tuscaloosa, AL 35487, USA; [7]Department of Earth Sciences, University of Connecticut, Storrs, CT 06269, USA; [8]Department of Biology, California State University Northridge, Northridge, CA 91330, USA

Author for correspondence:
Karolina Heyduk
Email: karolina.heyduk@uconn.edu

Received: *7 October 2024*
Accepted: *30 June 2025*

New Phytologist (2025)
doi: 10.1111/nph.70437

Key words: CAM, ecophysiology, Joshua tree, Mojave, photosynthesis, Yucca.

Summary

- Joshua trees are long-lived perennial monocots native to the Mojave Desert in North America. Composed of two species, *Yucca brevifolia* and *Y. jaegeriana* (Asparagaceae), Joshua trees are imperiled by climate change, with decreases in suitable habitat predicted under future climate change scenarios. Relatively little is understood about the ecophysiology of Joshua trees across their range, including the extent to which populations are locally adapted or phenotypically plastic to environmental stress.
- Plants in our common gardens showed evidence of Crassulacean acid metabolism photosynthesis (CAM) in a pilot experiment, despite no prior report of this photosynthetic pathway in these species. We further studied the variation and strength of CAM within a single common garden, measuring seedlings representing populations across the range of the two species.
- A combination of physiology and transcriptomic data showed low levels of CAM that varied across populations but were unrelated to home environmental conditions. Gene expression confirmed CAM activity and further suggested differences in carbon and nitrogen metabolism between *Y. brevifolia* and *Y. jaegeriana.*
- Together the results suggest greater physiological diversity between these species than initially expected, particularly at the seedling stage, with implications for future survival of Joshua trees under a warming climate.

Introduction

While desert species are often considered to be well adapted to many environmental 'extremes' – including drought and increasing temperatures – they are by no means impervious to the changing global climate. For example, the southwestern deserts of North America have experienced rising temperatures and a greater risk of extreme drought (Williams *et al.*, 2022), with dramatic and potentially negative consequences on both the flora and fauna of these regions (Archer & Predick, 2008; Munson *et al.*, 2012; Smith *et al.*, 2023). Climate change to date has driven substantial shifts in desert plants' phenology (Zachmann *et al.*, 2021), plant community composition (Munson *et al.*, 2012), and total vegetation cover (Hantson *et al.*, 2021). Iconic species like saguaro cactus (*Carnegiea gigantea*) are threatened by increasing drought that is predicted to hinder seedling recruitment (Félix-Burruel *et al.*, 2024). Because many desert species are long-lived perennials, determining their potential response to a changing global climate requires a better understanding of the degree to which they can respond to environmental pressures in the short term (e.g. plasticity), across life stages (e.g. demographically), or over evolutionary timescales (e.g. adaptation).

Observational studies that quantify extant diversity across the landscape cannot alone determine the effects of genetics, environment, or their combination (G×E). For example, saguaro cactus populations inhabiting extremes along a moisture gradient have significant differences in branching architecture that are correlated to water stress (Yeaton *et al.*, 1980), but whether branching structure differences were driven solely by environmental pressures, through genetic differences, or both is difficult to determine. By contrast, common garden studies, especially those that involve multiple gardens across the landscape, have the power to disentangle environmental and genetic contributions to trait variation in natural plant populations (Ebeling *et al.*, 2011;

Schwinning *et al.*, 2022). In two common Mojave Desert perennials, *Ambrosia dumosa* and *Larrea tridentata*, multiple common gardens representing different precipitation regimes were used to compare patterns of local adaptation in populations of both species (Custer *et al.*, 2022). *Larrea tridentata* and *A. dumosa* exhibited different mechanisms of coping with dry desert conditions, via avoidance of hydraulic failure and modulation of water use efficiency, respectively, highlighting the complex ways that perennial plants can adapt to the environment and the importance of common garden studies for determining the degree of adaptation and plasticity.

Eastern and western Joshua trees (*Yucca jaegeriana* McKelvey and *Y. brevifolia* Engelm., respectively) are sister species and are long-lived arborescent succulents (family Asparagaceae) endemic to the Mojave Desert ecoregion spanning southern California, southern Nevada, southwestern Utah, and northwestern Arizona (Esque *et al.*, 2023). Joshua trees are well known for their specialized moth pollination system (Pellmyr & Segraves, 2003; Godsoe *et al.*, 2008), and *Y. jaegeriana* and *Y. brevifolia* are associated with sister species of pollinating yucca moths, *Tegeticula antithetica* and *T. synthetica*, respectively (Cole *et al.*, 2017). The two species hybridize in a narrow zone of sympatry in south-central Nevada, but maintain detectable genetic differentiation thanks to geographic and pollinator-mediated isolation (Starr *et al.*, 2013; Yoder *et al.*, 2013; Royer *et al.*, 2016), and they have key morphological differences in leaf length and overall growth form (Lenz, 2007). Increasing land use changes in Joshua trees' habitats, wildfires, and a warming regional climate have prompted calls for federal protection (Smith *et al.*, 2023), and the western Joshua tree (*Y. brevifolia*) was recently protected by California state legislation (Western Joshua Tree Conservation Act, 2023).

Joshua trees' habitat experiences wide temperature swings both within a single day and across a growing season. In the cooler winter months, nighttime temperatures can drop well below freezing, while summer temperatures are often above 37°C. The Mojave Desert receives average annual precipitation totaling 130 mm (Hereford *et al.*, 2006), most of which falls during the winter. Climate in the western region of the Mojave Desert is generally wetter in the winter but drier in the summer, whereas the eastern Mojave Desert has more biannual rainfall patterns typical of the Sonoran Desert (Smith *et al.*, 1997). These differences between the eastern and western ends of the Mojave mean the two Joshua tree species occupy differing climate envelopes (Esque *et al.*, 2023). Physiological adaptations to these cold desert conditions have been well documented for Joshua trees. *Yucca brevifolia* was able to tolerate temperatures as low as −8.7°C, consistent with average low temperatures experienced in their range from year to year (Loik *et al.*, 2000). In addition to cold, the ecophysiology and leaf morphological traits in Joshua trees are thought to help these plants cope with high daytime temperatures. Heat-stressed *Y. brevifolia* seedlings grown at 53°C (relative to nominal conditions at 45°C) showed no significant reduction in photosynthetic assimilation rate (Huxman *et al.*, 1998). The newly developing leaves on Joshua tree leaf rosettes are often at an acute angle relative to the rosette stem, potentially allowing for greater light interception at times favorable to photosynthesis, either early/late in the day or during parts of the year when the sun is lower in the sky (Rasmuson *et al.*, 1994). A recent study demonstrated *Y. brevifolia*'s ability to quickly respond to water pulses via increased photosynthesis, even during the hottest part of the year (Hastings & Loik, 2025).

Extensive research has been done on the photosynthetic physiology of several *Yucca* species, including Joshua trees. Of the *c.* 50 species in the genus *Yucca*, roughly half are expected to use Crassulacean acid metabolism (hereafter CAM photosynthesis or CAM) based on carbon isotope ratio values (Heyduk *et al.*, 2016). CAM photosynthesis is a modification to the more common C_3 pathway whereby plants restrict most gas exchange to the night to avoid excessive evapotranspiration during the day. CAM acts as a carbon concentrating mechanism, sequestering nocturnal CO_2 as malate in the vacuoles of photosynthetic cells, then releasing and decarboxylating it during the day behind closed stomata. As a result, RuBisCO in CAM plants is surrounded by high concentrations of CO_2, and photorespiratory stress in CAM plants is believed to be reduced. CAM activity can range from constitutive, where plants rely on CAM for the majority of their carbon gain, to weak CAM, where plants obtain only a small proportion of their net carbon gain through the CAM cycle. In some weak CAM species, no atmospheric CO_2 is used at all, and instead, respired CO_2 is refixed by the CAM cycle. The benefit of CAM is therefore twofold: CAM reduces photorespiratory energy loss while minimizing water loss to the atmosphere.

Unsurprisingly, CAM is found in many arid-adapted plant species, including those in *Yucca* and *Agave*. However, prior work demonstrated *Y. brevifolia* is a C_3 species with no discernable nocturnal gas exchange indicative of CAM photosynthesis (though data are not shown in the publication) (Smith *et al.*, 1983), and subsequent studies did not further examine nocturnal photosynthetic activity (Huxman *et al.*, 1998). Joshua trees' position as taxa sister to the rest of the genus *Yucca* (Pellmyr *et al.*, 2007; Smith *et al.*, 2008, 2021; Heyduk *et al.*, 2016; McKain *et al.*, 2016), and their use of C_3 photosynthesis, was the basis for inferring a single and independent origin of CAM in one section of the genus (Heyduk *et al.*, 2016). Species of *Yucca* that differ in their photosynthetic pathway – like *Y. schidigera* Roezl ex Ortgies (CAM) and *Y. brevifolia* (presumably C_3) – are often found in the same habitat, raising questions about the evolutionary history of photosynthetic pathways in the genus as it relates to historical climates and biogeography. It should also be noted that the majority of species in the genus have not had photosynthetic physiology studied beyond carbon isotope ratios, which are known to mischaracterize weaker forms of CAM (Gilman *et al.*, 2023).

Despite the ecophysiological adaptations that allow Joshua trees to inhabit the arid environment of the Mojave Desert, modeling under future climate change scenarios paints an uncertain picture for the survival of these iconic desert species. Joshua trees currently inhabit a relatively narrow band of suitable environments, thought to be limited on one end by minimum survivable temperature and on the other by extreme heat events (Dole *et al.*, 2003). Within Joshua Tree National Park, models

Table 1 Sampling information across source populations of Joshua tree species, *Yucca brevifolia* and *Y. jaegeriana*.

Species	Population	Code	Elev (m)	MAP[1] (mm)	MAT[2] (C)	*n* (2022)[3]	No. of mat[4]
Yucca brevifolia	Upper Lancaster Rd	UL	925.3589	338	15.3	5	4
Yucca brevifolia	Lower Walker Pass	LWP	1326.568	251	13.8	5	5
Yucca brevifolia	Lower Montzuma Peak	LMP	1519.636	131	11.7	4	3
Yucca brevifolia	Upper Burns Canyon	HBC	2171.756	595	8.5	3	2
Yucca brevifolia	Upper Yucca Valley	UYV	1861.88	560	10.3	3	3
Yucca brevifolia	Lower Yucca Valley	LYV	1108.662	290	15.9	3	2
Yucca jaegeriana	Lower Cold Creek	LCC	1100.749	149	15.5	5	3
Yucca jaegeriana	Upper Cold Creek	UCC	1100.749	149	15.5	4	3
Hybrid	Tikaboo Valley	TV	1409.762	204	12.6	3	3
Yucca jaegeriana	Crystal Springs	CS	1676.715	256	10.9	5	4
Yucca jaegeriana	Lower Alamo Rd	LAR	635.2674	188	19.2	5	3
Yucca jaegeriana	Mid Meadview	MMV	1186.652	214	15.7	5	5
Yucca jaegeriana	Lower Meadview	LMV	953.343	184	17.2	5	3
Yucca jaegeriana	Upper Meadview	UMV	1676.055	316	12.3	4	4
Yucca jaegeriana	Upper Chicken Spring Rd	UCS	1152.208	289	15.9	5	4

[1]MAP: mean annual precipitation from BioClim.
[2]MAT: mean annual temperature from BioClim.
[3]Number of individuals sampled in 2022 per source population.
[4]Number of unique matrilines sampled per source population.

assuming minimal climate change mitigation predicted nearly no suitable habitat for the namesake species within the National Park by the end of the century; even models with mitigation resulted in < 20% of current-day habitat as refugia (Sweet *et al.*, 2019). Modeled results were supported by empirical demographic data collected in the park, which showed higher demographic recruitment by Joshua trees growing closer to predicted refugia (Sweet *et al.*, 2019). Climate threats are not only a future consideration; niche models for new recruits and adults in the area in and around Joshua Tree National Park found a near match between new recruits' niche model and a model based on a +1°C temperature change for adults (many of which were established 50–100 yr ago), indicating that climate change is already affecting demography and recruitment of Joshua trees (Barrows & Murphy-Mariscal, 2012). More broadly across the Mojave Desert, future suitable habitat models show significant decreases in the predicted distribution of Joshua trees (Cole *et al.*, 2011). Only one study has found an increase in the predicted range of Joshua trees by factoring in the net positive effect elevated atmospheric CO_2 is predicted to have on freezing tolerance, resulting in a slight increase in the overall predicted range of Joshua trees (Dole *et al.*, 2003). Such models could be further improved by a better overall understanding of the underlying genetic and ecophysiological diversity within and between Joshua tree species.

We set out to understand Joshua trees' local adaptation vs phenotypic plasticity in response to environmental factors by collecting seeds from across both Joshua tree species' ranges and planting them in different common garden environments. However, an initial screen that included photosynthetic traits and proof-of-concept RNA sequencing found that our seedlings showed gene expression patterns consistent with the use of CAM photosynthesis. We subsequently altered our sampling design and more intensely sampled photosynthetic phenotypes and gene expression at a single common garden site during the day and night to ascertain whether Joshua trees can use CAM photosynthesis and whether the ability to use CAM varied across populations or between species. We find evidence of weak CAM photosynthesis that varies between populations, suggesting this photosynthetic pathway is a possible mechanism underlying ongoing local adaptation.

Materials and Methods

Seed sources and common gardens

Indehiscent fruits of Joshua trees (*Yucca jaegeriana* McKelvey and *Y. brevifolia* Engelm.) were collected from 15 populations across the Mojave Desert (Table 1; Fig. 1a) in July 2019, when infructescences were senescing and pods were drying. Seeds were separated from fruits, air-dried, and stored in the laboratory in paper envelopes until propagation in the glasshouse.

A cohort of Joshua trees was propagated in the glasshouse for outplanting during summer and autumn 2020, but due to dramatically reduced survival in the gardens during prolonged drought (Williams *et al.*, 2022), a second cohort was propagated and outplanted during autumn 2021. Between August–September 2020, seeds for the first cohort were initially sown in flats with a 2 : 1 : 1 mixture of washed sand, perlite, and organic mulch, but seedling emergence was low. Seeds were subsequently incubated on Petri plates at 25°C from October to November 2020; Joshua tree seeds are nondormant (Reynolds *et al.*, 2012) and germinated within 2–5 d after imbibing water. All seedlings from flats and germinants from plates, respectively, were transplanted to Zipset™ plant bands (Stuewe & Sons, Inc., OR, USA) using the same soil mixture as in the flats. The second cohort of seedlings was incubated on Petri plates as before and transplanted to plant bands between September–November 2021. Seedlings

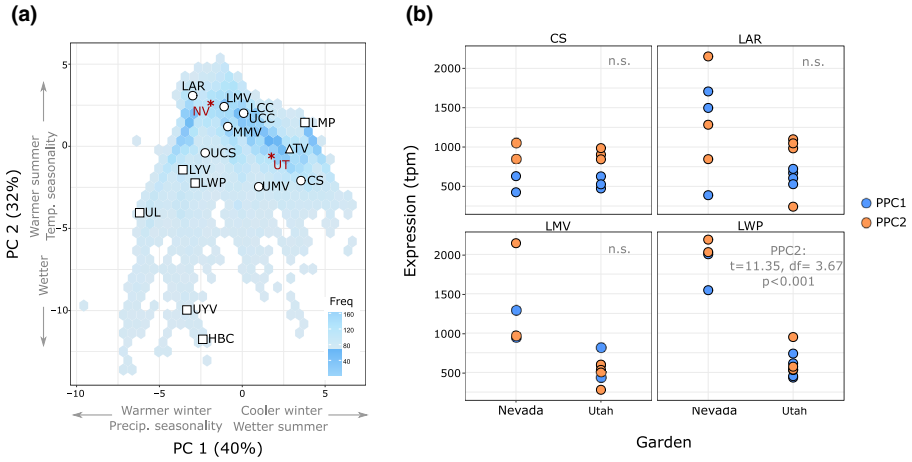

Fig. 1 Variation in home climate and results from a preliminary screen of source populations of Joshua trees. (a) First two principal component axes of climate variation for natural Joshua tree populations, showing frequency of Joshua tree occurrences across climate PCA space. Background frequency plot based on occurrence data in Esque *et al*. (2023). PC coordinates of source populations are labeled, with shape indicative of species (square: western Joshua tree (*Yucca brevifolia*), circle: eastern (*Yucca jaegeriana*), triangle: hybrid). Garden locations in climate space are indicated by red stars. (b) Daytime expression of phosphoenolpyruvate carboxylase (PPC) copies 1 and 2 from individuals from four source populations (CS, LAR, LMV, and LWP) sampled in two common gardens (Nevada, UT). The expression shown is based on mapping to the *Y. jaegeriana* reference transcripts and is shown for the PPC1 and PPC2 genes that were differentially expressed between gardens. In *post hoc t-tests* between gardens within each source population, only PPC2 showed differential expression, and only in LWP individuals; all other source population were not significantly different in expression between gardens (n.s.).

for both cohorts were watered weekly once established in plant bands until they were outplanted to the gardens.

Seedlings were moved to a shade house to acclimate to early spring conditions for 1 month before planting in gardens. Seedlings from each source population and matriline were stratified by number of leaves (range = 1 to 9 for both cohorts) and randomly assigned to each common garden so that variability in size was represented between gardens. The approximate age of seedlings at outplanting ranged from 4 to 7 months (2020 cohort) and 4–5 months (2021 cohort) (Fig. 1b). Seedlings were planted at a garden outside Searchlight, NV (hereafter NV garden) on 1–2 March 2021 and on 14–15 February 2022; seedlings were planted at a second garden near St George, UT (hereafter UT garden) on 10–11 March 2021 and 17–18 February 2022. Both gardens were previously fenced with a minimum 1.5 m tall metal mesh buried to a depth of 45 cm with metal flashing surrounding the top of the fence to minimize small mammal access. Seedlings were planted in holes spaced 50–75 cm apart, deeper than the 25 cm depth of the plant band, and at least 10 cm wide. Soils at each garden were dry to a depth of 25 cm due to prolonged drought conditions, so holes were moistened before planting, and moist soil from the hole was backfilled to ensure firm soil-to-root contact. The entire footprint of the planting area was subsequently watered by overhead spray to maintain moisture in the soil profile through the first summer. Supplemental watering at the NV garden was a rainfall-equivalent of 107 mm (plus 31 mm of rain) through 13 September 2021 for the 2020 cohort and 107 mm rainfall-equivalent (plus 88 mm rain) through 29 August 2022 for the 2021 cohort. The UT garden received a rainfall-equivalent of 48 mm (plus 102 mm rainfall) through 24 August 2021 and 214 mm rainfall-equivalent (plus 59 mm rain) through 6 September 2022. Seedlings were monitored monthly for growth and survival. Garden weeds were removed by hand, and when seedlings had signs of herbivory, seedlings were covered with protective mesh cages.

Preliminary RNA sampling (2021)

In June 2021, plants in the two common gardens were used as a test for protocols and procedures. Leaves were taken for preliminary tests of RNA sampling protocols; samples were obtained from 15 plants from 4 source populations (CS $n = 3$; LAR, LMV, and LWP $n = 4$) at the UT garden, and from 9 plants from the same source populations (CS, LMV, and LWP $n = 2$; LAR $n = 3$) at the NV garden. Leaf samples were collected midmorning at each location, cut lengthwise in half to increase the amount of exposed inner tissue, and were placed in 1 ml of RNA stabilization reagent (RNAlater™) solution (Thermo Fisher Scientific, Waltham, MA, USA). To test the effects of sample storage conditions on RNA quality, a subset of RNA tissue in RNAlater from the NV garden was kept at ambient temperatures for *c.* 1 wk, while RNA samples from the remaining NV individuals and the UT garden were kept on ice. All samples were then frozen at −80°C until further processing.

RNA was extracted from RNAlater leaf samples using RNeasy Plant Mini Kits (Qiagen, Germantown, MD, USA), purified with Ambion Turbo DNAse™ treatment per manufacturer's protocol, and quantified via Qubit® High Sensitivity (HS) RNA assays (Thermo Fisher Scientific). Sequencing libraries were prepared from RNA samples using KAPA (Roche, Indianapolis, IN, USA) mRNA stranded kits at half reaction, using custom-ordered combinatorial dual barcodes from BadDNA (http://baddna.uga.edu/). Libraries were quantified by both Qubit HS DNA assays and real-time PCR using Kapa's Illumina

standards. Libraries were sequenced at the University of Oregon Genomics & Cell Characterization Core Facility on a NovaSeq™ 6000 SP flow cell (Illumina, San Diego, CA, USA) with 150 bp paired-end reads, targeting 10–15 million reads per library.

RNA analysis (2021)

In general, samples kept in RNAlater on ice had better RNA and downstream library quality than samples kept at ambient temperatures for 1 wk (data not shown). RNA reads were cleaned with Trimmomatic v.0.36 (Bolger *et al.*, 2014) and mapped to a preliminary annotation of the *Yucca jaegeriana* genome using only primary transcripts (the coding sequences (CDS; available on Dryad) with kallisto (Bray *et al.*, 2016) and analyzed with sleuth (Pimentel *et al.*, 2017)). Differential expression analysis between source populations and between gardens was conducted with the likelihood ratio test framework in sleuth, whereby one variable is removed from the model while keeping the other. In the resulting lists of differentially expressed genes, one gene in particular was a surprise: *phosphoenolpyruvate carboxylase* (*PPC*). This protein interacts with the citric acid cycle in most plants by supplying intermediate metabolites. However, it is also recruited for CAM photosynthesis as the major carboxylation enzyme. Expression of *PPC* in the preliminary RNA-seq data was higher than would be expected for a general maintenance gene in a strictly C_3 species, based on previous analyses within the Agavoideae (Heyduk *et al.*, 2022). As a result, we shifted our focus to determining if CAM photosynthesis is present in Joshua tree seedlings, despite previous evidence suggesting *Y. brevifolia* is C_3 (Huxman *et al.*, 1998).

Garden sampling (2022)

To determine whether Joshua trees use CAM, we redesigned our following year's sampling design. Due to high mortality in the gardens during summer 2021, only the UT garden had enough seedlings for sampling the following year. In May 2022, we measured photosynthesis and collected tissue for RNA sequencing on 72 plants from the UT garden, representing 15 source populations (full numbers of replicates per source population can be found in Table 1). Six populations were true western Joshua trees (*Yucca brevifolia*), another eight were true eastern (*Yucca jaegeriana*), and one population was sampled from the hybridization zone (Starr *et al.*, 2013). The three maternal plants in the hybrid zone whose offspring were sampled in the common gardens were previously genotyped and had 0.57, 0.62, and 0.88 proportions of *Y. brevifolia* ancestry (Starr *et al.*, 2013). At 9:30 am local time (*c.* 3 h after sunrise), we measured photosynthetic rates with both a LI-6400XT and a LI-6800 (LI-COR Environmental, Lincoln, NE, USA) simultaneously to measure all 72 plants within a reasonable time frame (*c.* 3 h). As plants were randomized in the garden, the two LI-COR instruments measured essentially a random mix of individuals from source populations, and subsequent analysis showed no significant difference between instruments (data not shown). During measurements, CO_2 in the chamber was set to 420 ppm, light was kept constant at 1800 μmol m^{-2} s^{-1}, and temperature was changed to track ambient as the morning progressed and ranged from 23 to 28°C during the day. Fan speed was set to 10 000 for the LI-6800 and the max setting for the 6400; flow rates of 400–500 were used on both machines. Tissue for RNA was sampled at the same time as morning photosynthetic measurements as in 2021: samples were placed directly into *c.* 1 ml of RNAlater and kept cool on ice until placed in a freezer. At dusk (18:30 h local, *c.* 2 h before sunset), leaf samples were cut and immediately placed on dry ice to be used for titratable acidity measurements to test for CAM activity.

Nighttime measurements followed a similar pattern to the daytime. At 21:30 h (*c.* 1 h after sunset), leaf photosynthesis was measured again, and leaf samples were again taken for RNA-seq. For photosynthesis measurements, no light was used in the chamber, and the temperature was again set to track ambient and ranged from 22 to 12°C. Finally, at 15:30 h (*c.* 3 h before sunrise), we sampled tissue for titratable acidity as in the daytime. The leaf used for photosynthetic measurements in both day and night times was harvested for leaf area, saturated and relative water content (SWC and RWC), and carbon isotope ratio measurements. Leaves were placed in pre-weighed screw-top vials and transported to the lab, where the leaf plus vial was weighed; deionized water was then added to the vial with the cut leaf submerged in the water. After 24 h, the leaves were patted dry, and the saturated tissue was weighed. The difference between the field-collected and imbibed masses was used to calculate RWC. After reweighing, the leaves were pressed between two glass plates to make an image of leaf area using diazo paper; the image was passed through a scanner, and leaf area was recorded (WinFolio, Regent Instruments, Inc., Québec City, QC, Canada). Subsequently, the leaves were dried on silica beads for carbon isotope analysis. RNA-seq and titratable acidity tissue samples were frozen at −80°C until they were shipped to the University of Hawai'i at Mānoa for further processing.

Carbon and nitrogen isotopes

Leaves used for RWC analysis were stored long-term on silica; *c.* 1 cm long pieces were shipped to the University of Connecticut in summer 2023, where they were further oven dried for 1 wk at 60°C. Tissue was then hand-ground by mortar and pestle into a fine powder. Organic geochemical measurements were performed at the Stable Isotope and Organic Molecular Biogeochemistry Laboratory at the University of Connecticut. Approximately 0.5–1 mg of dried and powdered plant tissue was weighed in 3.5 × 5 mm tin capsules for isotopes via continuous flow using a 4010 Elemental Analyzer (Costech Analytical, Valencia, CA, USA) coupled with a Thermo Scientific MAT 253 Plus gas isotope ratio mass spectrometer (EA-IRMS). Measured isotope values were corrected for mass scale, size, and drift effects using a suite of international isotope reference standards that span the range of isotopic compositions observed in our samples: caffeine (IAEA-600), sucrose (IAEA-CH-6: 8542), and L-glutamic acid (USGS40: 8573). The SD of the residuals of the reference materials was 0.15‰, and the SE of the residuals was 0.01‰. All

carbon isotope (δ13C) values are reported in per mil (‰) relative to Vienna Pee Dee Belemnite (VPDB) in standard delta notation. Leaf nitrogen content was calculated as the mass of N relative to the mass of tissue analyzed.

Maternal plant titratable acidity

Maternal plants of a subset of seedlings were sampled in May 2023 for acid titration measurements. Individuals from six source populations, of which three had offspring planted in our common gardens, were sampled at dawn and dusk; tissue was immediately frozen in a dry shipper until placement in cold storage.

Titratable acidity measurements

Frozen tissue from garden seedlings and maternal samples was weighed before being added to 60 ml of 20% ethanol. Leaf titrations were completed following protocols from Heyduk *et al.* (2021). In brief, the solution was boiled until reduced by half and then returned to 60 ml by adding deionized water. The boiling and water addition process was completed again, and then the solution was left to cool down to room temperature. Leaves were then removed from beakers, and the solution was titrated with 0.002 M NaOH up to a pH of 7.0 using a pH meter. The µl quantity of NaOH used for titrations was recorded for each sample and was converted into µmol of H+ according to the following equation used in Heyduk *et al.* (2021): (ml of 0.002 M NaOH × 2 mM)/grams of leaf tissue.

Citrate measurements

Leaf citrate content was measured from glasshouse-grown plants of both nonhybrid species using an enzymatic colorimetric assay. Seeds of glasshouse-grown plants were initially collected at the same time as the seeds for our common gardens. Seeds were germinated in summer 2023 via Petri dishes as previously described, then planted in tree pots that measured 4″ in width and 14″ in depth, and grown at the University of Connecticut glasshouses. Soil was a mixture of 60% sand to 40% Pro-Mix® BX (Premier Tech Ltd., Rivière-du-Loup, QC, Canada). Plants were kept well-watered and were randomized in their location on the bench relative to the source population. In 2024, three seedlings were sampled for each of three source populations of eastern (*Y. jaegeriana*; populations LYV, HBC, LMP) and western (*Y. brevifolia*; CS, LAR, UCS). Tissue was collected shortly after dawn (*c.* 8 : 00 h) and shortly before dusk (*c.* 16:00 h) and flash frozen in liquid N_2, then stored in a −70°C freezer until processing.

For the citrate assay, each leaf sample was ground by hand in liquid N2 with a mortar and pestle to a fine powder. Approximately 10–50 mg of ground tissue was resuspended with 500 µl of phosphate-buffered saline and centrifuged at 10 000 **g** for 10 min The supernatant was then used as input for a citrate assay kit (Sigma-Aldrich) using kit instructions. Samples were evaluated at full and half sample volume (half concentration) to ensure measured values were within the standard range. The concentration of citrate in samples was estimated per kit instructions and normalized by the tissue input weight. The average value from the two technical replicates (at full and half concentration) was used for further analyses.

Statistical analyses

Photosynthetic measurements and values of titratable acidity can be noisy; individual outlier values greater than two SD from the mean of each trait were removed from both measurement types. In most instances, these outliers represented biologically unrealistic values (e.g. a photosynthetic rate of 30 µmol m^{-2} s^{-1} during the day in a juvenile desert perennial). Additionally, because Joshua tree leaves are relatively thick even at the seedling stage, 18 (out of 64) measurements taken with the LI-6800 had flow leaks of *c.* 50% – these were removed from further analyses. A flow leak measurement is not available on the 6400, and we instead removed samples that had impossible Ci values (negative), as well as a set of measurements where CO_2 was set to 500 instead of 420 ppm; a total of 23 out of 74 measurements with the 6400 were removed from further analyses. To test the effect of each plan's home environment on measured physiological traits and gene expression, we used a principal components analysis (PCA) to generate major axes of variation in the climate space of each source population of Joshua trees used for this study along with a broad survey of Joshua tree individuals across the range from both field observations and from satellite imagery (a subset of 10 000 data points from the latter, randomly drawn) (Esque *et al.*, 2023) (Fig. 1a).

We downloaded the 19 BioClim climate variables, averaged over 1970–2000, for the 10 000 random points within the geographic range (Fick & Hijmans, 2017). We then summarized variation in the 19 BioClim variables using the prcomp() function in R. The first principal component (PC) explained 40% of the variation and separated sites with warmer temperatures and drier summers from sites with cooler temperatures and more summer precipitation; the second PC explained 32% of the variation and separated warmer, drier climates with greater seasonal variation in temperature from cooler, wetter climates with less seasonal temperature variation; the third PC explained 11% of the variation, separating climates with wider daily and annual ranges of temperature from less widely varying climates. In R (R Core Team, 2024), using the lmer() function from the package lme4, linear mixed-effect models were generated that tested for the change in titratable acidity, night and daytime assimilation rates, SWC, RWC, and carbon isotope ratio in response to fixed effects of all three climate axes and whether each plant was *Y. brevifolia, Y. jaegeriana*, or a hybrid. Elevation was excluded from our models due to high collinearity with other factors (as determined by an adjusted generalized variance inflation factor > 3). The matriline of each seedling was included as a random effect. The drop1() function (likelihood ratio test) was used to sequentially test the effect of dropping each fixed parameter, one at a time.

RNA analysis (2022)

Leaf tissue samples harvested for RNA analysis were ground by hand in liquid nitrogen using a mortar and pestle. RNA was

extracted following the protocol above (for the 2021 RNA samples). Final sequencing was conducted at the University of Connecticut Center for Genome Innovation on a NextSeqTM 500 (Illumina) with 150 bp reads, targeting *c.* 10–20 million pairs of reads per library. Sequences were cleaned in TRIMMOMATIC v.0.39 (Bolger *et al.*, 2014) then mapped to the preliminary annotation of the *Yucca jaegeriana* genome (against only primary transcripts) using kallisto (Bray *et al.*, 2016) and analyzed via sleuth (Pimentel *et al.*, 2017). Sleuth implements a strict filtering step by default that requires at least five counts in 47% of libraries; we modified this filter to allow for more presence/absence across our experimental design by lowering the threshold to only 25% of libraries with at least five counts. Time of day, source population, and species were all used as factors in model testing (with likelihood ratio tests) and were tested both additively and interactively, using built-in Benjamini–Hochberg multiple test correction in sleuth. Hybrid individuals were treated as a third species in our model testing, though they had a low sample size of only three individuals. We used OrthoFinder (Emms & Kelly, 2019) to generate functional annotations based on sequence similarity of *Y. jaegeriana* coding sequences to reference angiosperm annotations. Reference genomes were downloaded from Phytozome (Goodstein *et al.*, 2012) and included in the OrthoFinder analysis: *Ananas comosus* v3 (Ming *et al.*, 2015), *Asparagus officinalis* v1.1 (Harkess *et al.*, 2017), *Arabidopsis thaliana* Araport11 (Cheng *et al.*, 2017), *Amborella trichopoda* v1.0 (Amborella Genome Project, 2013), *Brachypodium distachyon* v3.1 (International Brachypodium Initiative, 2010), *Musa acuminata* v1 (D'Hont *et al.*, 2012), *Oryza sativa* v7 (Ouyang *et al.*, 2007), *Sorghum bicolor* v3.1.1 (McCormick *et al.*, 2018), *Setaria italica* v2.2 (Bennetzen *et al.*, 2012), *Yucca aloifolia* v2.1, and *Yucca filamentosa* v2.1.

Results

Our preliminary sampling in 2021 revealed signals of CAM photosynthesis in Joshua tree seedlings based on gene expression, despite no prior indication that this species uses CAM. Our sampling across the two species was not sufficient to assess differences between them. Subsequent detailed photosynthetic phenotyping and comparisons between daytime and nighttime gene expression confirmed CAM photosynthesis activity across populations of Joshua trees to varying degrees. However, we found that neither the level of CAM activity nor other physiological phenotypes were explained by the source population's home climate. Gene expression showed strong differences between time points and, perhaps more surprisingly, strong differentiation between species, vincluding in pathways related to carbon and nitrogen metabolism.

Preliminary sampling in 2021

RNA-seq data were tested for significant garden effects (n = 9033 transcripts at q value ≤ 0.05), significant source population effects (n = 1529), or the interaction of garden and source population (n = 9) (annotated lists available in Supporting Information Table S1). These results were not further investigated as this was a preliminary proof-of-concept experiment, with the exception of noting that a copy of *PPC* was one of the transcripts that had significant garden effects ($X^2(1) = 9.03$, $q = 0.014$): on average, expression was higher in the NV garden plants relative to the UT plants (Fig. 1b) though this was entirely driven by LWP individuals (Fig. 1b). PPC is important in all plants for providing metabolic intermediates to the citric acid cycle, and its expression can be affected by environmental cues (Lepiniec *et al.*, 1994; Chollet *et al.*, 1996). Gene copies of *PPC* get recruited for novel photosynthetic functions in CAM and C_4 plants (Heyduk *et al.*, 2019). However, the copy expressed differently in Joshua trees in different gardens is known as *PPC2* or the 'bacteria' version, named so for its homology to gene copies found in *E. coli* (O'Leary *et al.*, 2009). PPC2 is thought to be used for CAM photosynthetic function in other *Yucca* species (Heyduk *et al.*, 2022), as well as a distantly related, aquatic CAM lycophyte, *Isoetes taiwanensis* (Wickell *et al.*, 2021). The two common gardens used in 2021 were quite different in precipitation and temperature in the 6 months preceding measurement (January–June 2021): the Nevada garden was on average 2.9°C warmer in each month than Utah, and Utah received 101.6 mm of rainfall while Nevada only received 19.6 mm in the same period. While not definitive proof of CAM activity, the upregulated expression of *PPC2* and the general increase in its expression in the warmest garden in individuals from two source populations challenged the idea that Joshua trees rely on only C_3 photosynthesis.

Physiology from 2022 sampling

Gas exchange measurements taken during the day and at night in May 2022 revealed that some Joshua trees were C_3 + CAM, using both pathways to obtain carbon for photosynthesis (Fig. 2a,b). On average, daytime and nighttime assimilation rates were above zero ($t = 6.25$, df = 37, $P < 0.001$ for daytime; $t = 4.18$, df = 46, $P < 0.001$ for nighttime) across all individuals. Source population was not a significant explanatory factor in either assimilation measurement ($F_{12,24} = 1.114$, $P = 0.394$ for daytime; $F_{14,32} = 1.173$, $P = 0.341$ for nighttime) (Fig. 2a, b). In both assimilation measurements, there was no clear difference between western (*Y. brevifolia*) and eastern (*Y. jaegeriana*) species ($t = 1.28$, df = 24.1, $P = 0.213$ for daytime assimilation; $t = -1.53$, df = 18.1, $P = 0.143$ for nighttime assimilation). On average, nighttime acid accumulation was significantly greater than zero across all individuals ($t = 4.13$, df = 58, $P < 0.001$), though there was no difference between species for the total amount of accumulated leaf acids ($t = 1.16$, df = 41, $P = 0.25$) (Fig. 2c). Source population was again not a significant factor in explaining acid accumulation ($F_{14,44} = 0.862$, $P = 0.602$). The correlation between nocturnal CO_2 assimilation and acid accumulation was not tested, as the former was measured at a single time point that cannot be extrapolated to the entire amount of nocturnal CO_2 fixed. None of the climate axes or species designations were significant explanatory variables for the levels of titratable acidity, daytime assimilation, or nighttime

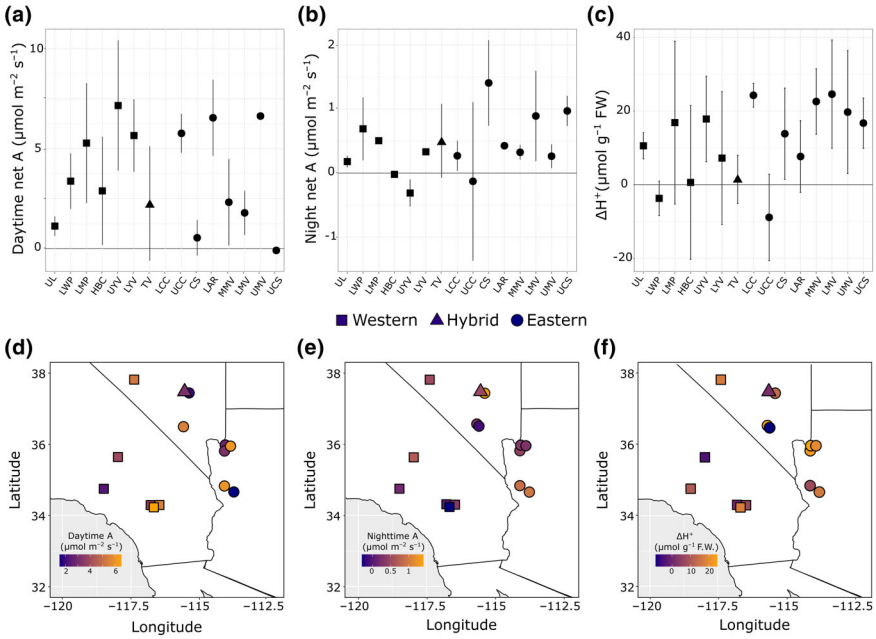

Fig. 2 Carbon assimilation and leaf acid accumulation in common garden-grown Joshua trees. Mean and SE of daytime assimilation of CO_2 (a), mean nighttime assimilation (b), and mean accumulation of leaf acid (delta H^+) (c). Means are shown across source populations, arranged first by species classification, then from west to east along the *x*-axis. Shapes correspond to classification as western Joshua trees (*Yucca brevifolia*), eastern Joshua trees (*Yucca jaegeriana*), or a hybrid between the two. (d–f) points on the map showing the location of each source population, shaded by mean population value for daytime photosynthesis (d), nighttime photosynthesis (e), and acid accumulation (f).

assimilation, with the exception of PC3 as a significant factor in daytime assimilation rate ($\beta = -1.18$, $X^2(1) = 4.74$, $P = 0.029$). Because *Y. brevifolia* and *Y. jaegeriana* are separate species (Royer *et al.*, 2016), we further tested within-species effects of climate PC axes, but no factor significantly explained any of the physiological traits measured.

Three metrics of water stress were measured in the common garden plants: relative water content (RWC) (Fig. 3a), saturated water content (SWC) (Fig. 3b), and carbon isotope ratio (Fig. 3c), an integrated measure of water-use efficiency (Fig. 3a–c). SWC had a narrow range from 1.37 to 2.98 and did not correlate to RWC; no explanatory variable in the model was significant in tests on all individuals or within eastern (*Y. jaegeriana*) samples, but PC3 was a significant factor in explaining SWC variation in western (*Y. brevifolia*) individuals ($\beta = -0.19$, $X^2(1) = 12.73$, $P < 0.001$). RWC was not significantly different across source populations, between species, nor was it explained by climate axes. Within species, RWC was not correlated to any other physiological trait, nor was it associated with any climate axes. Neither SWC nor RWC correlated significantly to any measures of photosynthesis (nighttime or daytime CO_2 uptake or titratable acidity, using Spearman's rank correlation).

Carbon isotope ratio was not significantly explained by any climate axis or species when testing all individuals together in a mixed-effect model; when testing the effects of the climate axis separately within the two nonhybrid species, PC3 was a significant factor for explaining carbon isotope ratio in the western Joshua tree (*Y. brevifolia*) ($\beta = -0.27$, $X^2(1) = 4.08$, $P = 0.043$). PC3 varies from cool, wet, and seasonal to warm, dry, and consistent, and counterintuitively suggests that plants from wetter habitats had greater water use efficiency in the common garden. However, it may also represent shifts in either water-use efficiency or the degree to which plants use CAM vs C_3 in the common garden environment (Messerschmid *et al.*, 2021).

The carbon isotope ratio was likewise not correlated to any other physiological measurement. The mean of all isotope values was −23.7‰, and a single individual plant (from the CS population) had an isotope value greater than −20.9‰, near the threshold −20‰ that has historically been used to separate C_3 from CAM species (Fig. 3c) (Gilman & Edwards, 2020). Leaf nitrogen percent varied from 0.3–3% but showed no association with PC climate axes, elevation, or the difference between species. All physiological data for garden-sampled individuals can be found in Table S2.

Finally, maternal plants sampled from six source populations showed variable amounts of leaf acid accumulation, translating to variable amounts of CAM activity (Fig. 3d). Individuals from LWP and HS had no significant accumulation of acids at night, while the remaining four populations had significant acid accumulation in maternal plants (Fig. 3d) (UWP: $t = 4.93$, df = 8, $P = 0.001$; CS: $t = 7.56$, df = 4, $P = 0.002$; LMV: $t = 4.22$, df = 5, $P = 0.008$; MV: $t = 3.44$, df = 6, $P = 0.014$). Unlike for offspring, the source population was a significant factor in predicting total acid accumulation ($F_{5,34} = 5.96$, $P < 0.001$). For those populations with both maternal plants and offspring in gardens sampled, offspring tended to have a similar range of values as maternal plants; correlations across matrilines were not possible due to a limited overlap in maternal matrilines sampled and matrilines represented by garden samples.

Gene expression differences

The effects of time of day, source population, and species were tested by comparing a reduced model with each factor dropped to a full model where the additive effect of all three factors was considered. Considering the source population, adding time of day to the model resulted in 16 197 significantly ($q \leq 0.05$) differentially expressed genes. The addition of the source population

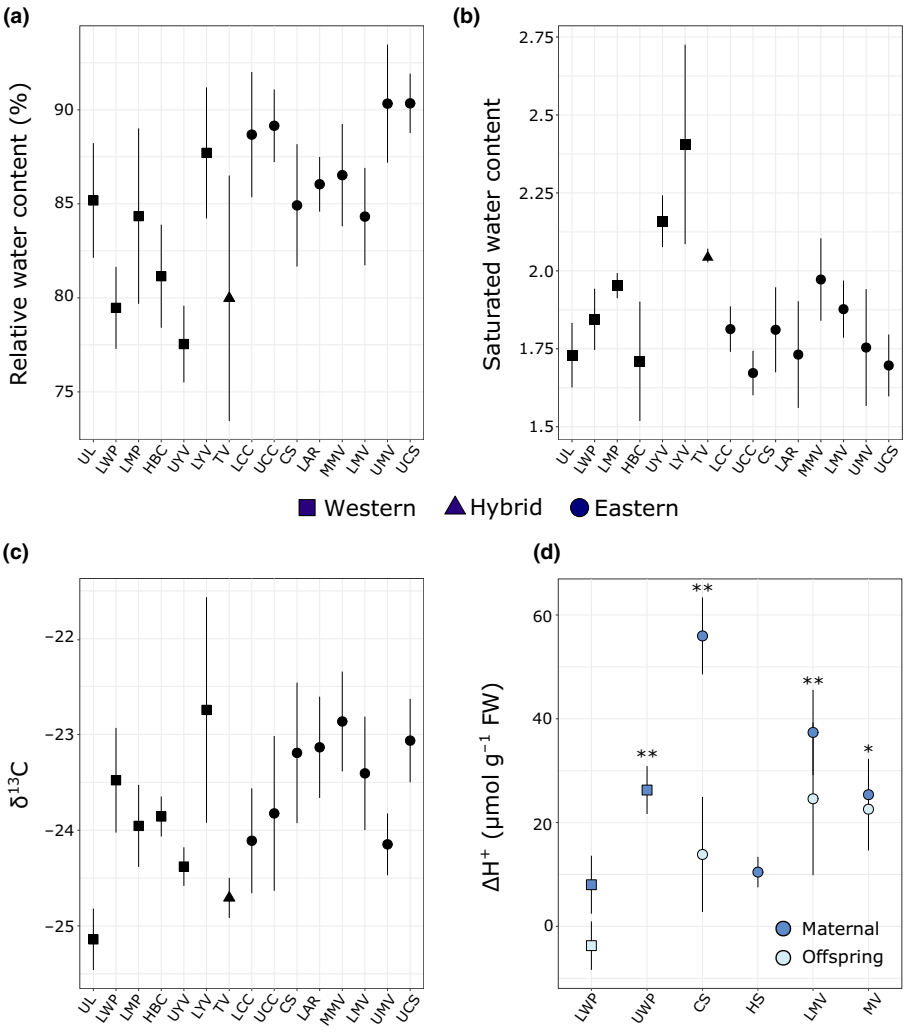

Fig. 3 Measures of water content, water use, and maternal adult plant leaf acidity. (a) Relative water content, (b) saturated water content, and (c) carbon isotope ratio means per population with SE for common garden plants. (d) Delta H^+ mean and SE calculated from titrations on maternal plant leaf tissue relative to offspring H^+ measurements from the common garden, where available. Significance values in (d) are from one-sample *t*-tests (dawn vs dusk H^+) and are indicated with asterisks: *, $P < 0.05$; **, $P < 0.01$.

to a model that took time of day into account resulted in 15 576 genes differentially expressed. Of these two sets, 9929 genes were significant in both, meaning they were differentially expressed between source populations and between timepoints. There was only one gene differentially expressed via an interaction of time and source population: a BTB/POZ domain-containing protein involved in ubiquitination pathways. We also tested the effect of species and time as factors as above: 14 064 genes were differentially expressed in response to time while taking species into account, while 9681 genes were differentially expressed in response to species while time was taken into account. A total of 5424 genes were significantly differentially expressed in response to both time and species. Only two genes had any interactive effect of time and species: the same BTB/POZ domain-containing protein and an ortholog to *Receptor-Like Protein 4*. A total of 14 060 genes were significant in response to time in both test frameworks (in other words, all genes differentially expressed by time with species taken into account were present in the list of genes when taking the source population into account). Similarly, many (8590 of 9681) genes differentially expressed between species were also differentially expressed between source populations. Lists of differentially expressed genes in these different comparisons can be found in Table S3.

Notable functions found in genes differentially expressed between species included those involved in auxin and ABA response, genes involved in chloroplast function and light sensing, and citrate metabolism. Cytosolic *isocitrate dehydrogenase* (*IDH*) showed high expression in eastern Joshua tree (*Y. jaegeriana*) samples but significantly lower expression in western Joshua trees (*Y. brevifolia*) (Fig. 4) ($X^2(2) = 190.28$, $q < 0.001$). IDH converts isocitrate to 2-oxoglutarate (2-OG), which can then either proceed through the citric acid cycle or can be shuttled into nitrogen metabolism through the GOGAT pathway. Indeed, other genes responsible for provisioning substrates for the citric acid cycle were also differentially expressed between species. Eastern Joshua tree (*Yucca jaegeriana*) had elevated expression of *pyruvate kinase* (*PK*) ($X^2(2) = 61.83$, $q < 0.001$), cytosolic *PPC* (the copy not used for CAM, based on expression pattern and levels) ($X^2(2) = 70.96$, $q < 0.001$), and *citrate synthase* (*CS*) ($X^2(2) = 53.86$, $q < 0.01$) (Fig. 4), and had significantly higher citrate content in the leaves than western (*Y. brevifolia*) individuals (Fig. 4; Table S4) ($t = -3.58$, df = 22.7, $P = 0.002$). Conversely, western individuals (*Y. brevifolia*) had elevated

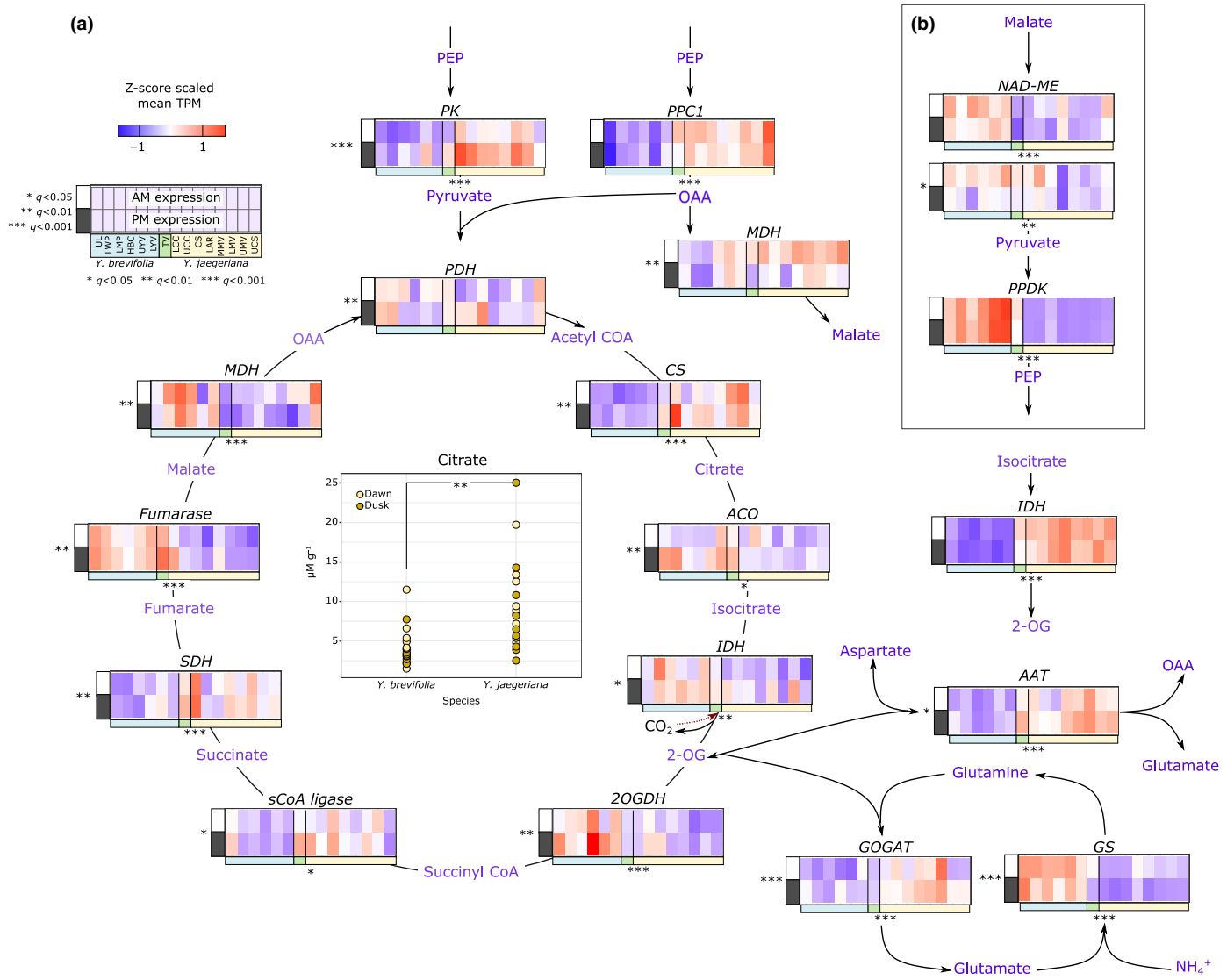

Fig. 4 Overview of the citric acid cycle in Joshua trees, showing connections between carbon and nitrogen metabolism via gene expression. Mean transcript z-score scaled TPM expression values per source population, with outliers (> 2 SD) removed, for (a) major citric acid cycle and nitrogen assimilation genes and (b) *PPDK* and upstream expression of *NAD-ME*. Expression is shown for both daytime and nighttime samples, indicated by open (day) and black (night) bars to the left of each heatmap. Source populations are arranged across the *x*-axis with western Joshua tree (*Yucca brevifolia*) populations to the left (blue), eastern (*Y. jaegeriana*) populations to the right (yellow), and the hybrid zone in the center (green), then arranged from west to east within each species. [Correction added on 17 September 2025, after first online publication: the terms 'eastern' and 'western' in the preceding sentence have been updated.] Dashed arrow below *IDH* indicates the possible reverse function of IDH. Genes shown are those that had the strongest between-species difference and are purported to be expressed in the correct cellular location, based on *Arabidopsis* annotation (e.g. citric acid cycle genes are expected to be expressed in the mitochondria). Asterisks indicate whether a transcript had significant differential expression between time points (left of plot) or between species (below plot). Metabolites or products are shown in purple text. Abundance of citrate is shown in the center; dawn and dusk samples are colored in different hues but were analyzed together when testing between species, as there was not a significant effect of time of sampling on concentration. 2OGDH, 2-oxoglutarate dehydrogenase; 2-OG, 2-oxoglutarate; AAT, aspartate aminotransferase; ACO, aconitase 3; CS, citrate synthase; GS, glutamine synthase; GOGAT, glutamine oxoglutarate aminotransferase; IDH, isocitrate dehydrogenase; MDH, malate dehydrogenase; NAD-ME, NAD malic enzyme; OAA, oxaloacetate; PDH, pyruvate dehydrogenase; PEP, phosphoenolpyruvate; PEPC, phosphoenolpyruvate carboxylase; PK, pyruvate kinase; PPDK, pyruvate orthophosphate dikinase; sCoA ligase, succinyl CoA ligase; SDH, succinate dehydrogenase.

expression of *2-OG dehydrogenase* (*2OGDH*) ($X^2(2) = 24.80$, $q < 0.001$), the enzyme responsible for converting 2-OG to succinyl-CoA within the citric acid cycle. Likewise, *fumarase* ($X^2(2) = 55.24$, $q < 0.001$) and mitochondrial *malate dehydrogenase* (*MDH*) ($X^2(2) = 24.97$, $q < 0.001$) were more highly expressed in *Y. brevifolia* (Fig. 4).

While not all genes in the citric acid cycle showed clear differential expression between species, genes that were differentially expressed suggest different carbon flux through the citric acid cycle between species of Joshua tree, further supported by elevated citrate levels in eastern (*Y. jaegeriana*) but not western (*Y. brevifolia*)If there are high levels of 2-OG produced by high

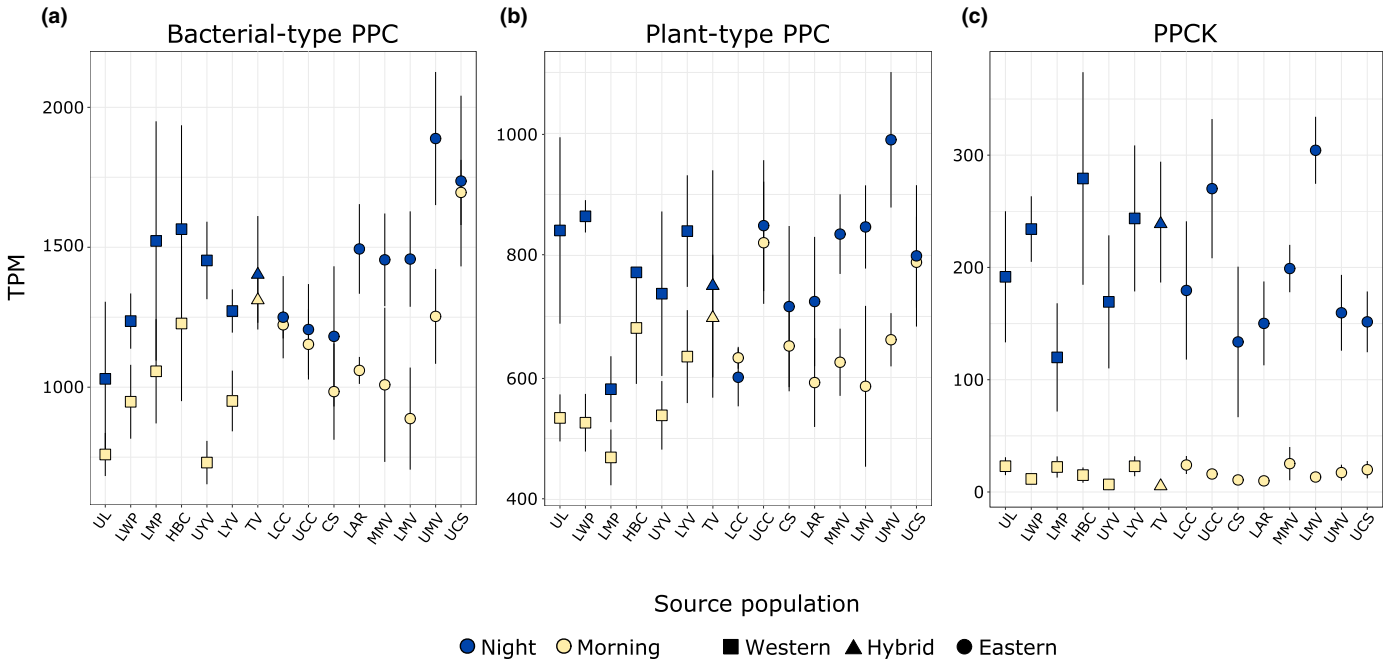

Fig. 5 Gene expression of photosynthetic transcripts in Joshua tree seedlings. Mean expression and SE (in transcripts per million) per population of samples taken at night and in the morning in bacterial-type (a) and plant-type (b) *phosphoenolpyruvate carboxylase* (*PPC*) and *PPC kinase* (*PPCK*) (c). Shapes correspond to classification as western Joshua trees (*Yucca brevifolia*), eastern Joshua trees (*Yucca jaegeriana*), or a hybrid between the two.

expression of *IDH* in eastern individuals (*Y. jaegeriana*), these could be siphoned off for amino acid production (supported by higher expression of both *glutamate synthase* (*GOGAT*) ($X^2(2) = 20.77$, $q < 0.001$) and *aspartate aminotransferase* (*AAT*) ($X^2(2) = 27.23$, $q < 0.001$) in *Y. jaegeriana* (Fig. 4)) or photorespiration (Fig. S1). Outside of the immediate citric acid cycle and nitrogen metabolism, *pyruvate, phosphate dikinase* (*PPDK*) is more highly expressed in western (*Y. brevifolia*) than eastern (*Y. jaegeriana*) individuals ($X^2(2) = 206.73$, $q < 0.001$) and was one of the most highly differentially expressed transcripts; *PPDK* interconverts pyruvate to PEP, though its directionality in Joshua trees measured here is unclear. PEP produced from this reaction could be used for carbohydrate production via gluconeogenesis, but expression of downstream gluconeogenesis enzymes, like a subunit of *glyceraldehyde 3-phosphate dehydrogenase* (*G3P*), was more highly expressed in eastern (*Y. jaegeriana*) individuals ($X^2(2) = 221.07$, $q < 0.001$). [Correction added on 17 September 2025, after first online publication: some of the uses of 'eastern' and 'western' in the preceding two sentences have been updated.]

CAM pathway gene expression

Both *PPC1* (plant *PEPC*) and *PPC2* (bacterial *PEPC*) were highly expressed at night in the majority of populations, and both genes had significantly different expression between timepoints ($X^2(2) = 8.29$, $q = 0.009$ for *PPC1*, $X^2(2) = 6.55$, $q = 0.020$) for (*PPC2*) (Fig. 5a,b). More so than the *PPC* copies, *phosphoenolpyruvate carboxylase kinase* (*PPCK*) – which phosphorylates PPC to reduce its inhibition by malic acid, an important post-translational modification for CAM (Taybi *et al.*, 2000) – had strongly induced nocturnal expression in all source populations ($X^2(2) = 175.67$, $q < 0.001$, gene is in top 50 most differentially expressed genes between timepoints) (Fig. 5c). Other genes thought to be central to CAM metabolism, like *MDH*, malate transporters, and *beta carbonic anhydrase*, all had overall low expression levels. Neither copy of *PPC* nor *PPCK* had a correlation between its expression and the amount of leaf acid accumulated or the nocturnal assimilation rate.

Discussion

Ecophysiology of Joshua trees

This study shows evidence that Joshua tree species use the CAM photosynthetic pathway even at the juvenile life stage, and that the strength and activity of CAM vary across source populations when grown in a common garden. The extent to which this variability is due to differential local adaptation or phenotypic plasticity cannot be determined by the results presented here, but nevertheless provides compelling data that can be used for future studies to understand intraspecific variation in CAM photosynthesis.

The strength of CAM on any given day can be affected by temperature, sunlight, and water availability (Haag-Kerwer *et al.*, 1992; Carter *et al.*, 1996; Winter *et al.*, 2008). While Joshua trees certainly exhibit low levels of CAM – both as juveniles and adults – the degree to which CAM expression is modulated in response to the environment in these species remains unclear. Because we measured the strength of CAM on a single day, it is not particularly surprising that the measured CAM activity did not correlate with the home environment. Moreover, little is understood about intraspecific variation in CAM traits and the extent to which variation is driven by local adaptation or

phenotypic plasticity (Ferrari *et al.*, 2020; Heyduk *et al.*, 2021). Analysis of CAM strength across a precipitation gradient in *Puya chilensis* did show increasing CAM with decreasing environmental moisture, but replication was limited to a single environmental sampling gradient (Quezada *et al.*, 2014), and it is unclear to what extent this is a plastic vs adaptive response. Similarly, in the bromeliad *Aechmea bromeliifolia*, individuals from dry and high-light environments had higher rates of CAM, demonstrated by greater acid accumulation and higher values of carbon isotope ratios (Scarano *et al.*, 2002). But because measurements were taken from the field, it is again unclear whether these differences across environments represent plasticity or adaptation. In Joshua tree, additional work assessing source populations in multiple common gardens with contrasting environmental conditions will help determine the level of plasticity in CAM function.

Our study also highlights the importance of considering the juvenile life stage. Joshua trees have a long (*c.* 50–70 yr) juvenile stage where they are more susceptible to environmental stress and herbivory (Esque *et al.*, 2015), and the use of CAM in young plants is not often considered. Many CAM species are thought to employ C_3 at least at the cotyledon phase, and perhaps longer (Nobel, 1988; Winter *et al.*, 2008; Niechayev *et al.*, 2023), with some taxa having a specific and predictable developmental progression from C_3 to CAM (Herppich *et al.*, 1992; Winter & Holtum, 2007; Winter, 2019). But like the varied CAM phenotypes that exist in mature plants, juvenile plants can modulate the extent of CAM usage. A time course study that measured photosynthesis for the first 120 d of plant development revealed that constitutively CAM species could adjust facultatively to water availability (Winter *et al.*, 2008). Multiple bromeliad species engage facultatively in CAM under drought stress in both juvenile and mature plants (Beltrán *et al.*, 2013). The ability to engage in low-level CAM activity in the juvenile phase seems particularly advantageous, as it would require limited anatomical and enzymatic investment, but would allow sustained growth during a particularly susceptible life phase. Our results demonstrate that not only are juvenile Joshua trees performing CAM (as well as adults in some populations), but that greater attention should be paid to the possibility of CAM activity in juvenile life stages of plants more broadly.

Physiological traits studied in the common garden were not significantly associated with any climatic factors from home environments. There are a number of possible reasons for this result: there may, for example, be a large amount of phenotypic plasticity in response to the common garden environment that cannot be detected in the current experimental design. Additional measurements from individuals at different common gardens would be required to parse the extent to which plasticity is shaping physiological responses in Joshua tree seedlings. There is also a large mismatch in the temporal span of our physiological sampling and climate variables from home environments; we measured physiological traits on a single day in a single year, while the Bioclim variables are averages over three decades, from 1970 to 2000 (Fick & Hijmans, 2017). Finally, our study is on seedlings 1 yr post-outplanting, during which seedlings were initially given supplemental water. As a result, phenotypic differences may have been minimized due to the generally beneficial initial growing environment (Custer, 2017; Germino *et al.*, 2019).

Gene expression differences in time and across populations

It has been well documented that a large proportion of all transcripts produced by a plant genome cycle in accordance with the circadian clock (Covington *et al.*, 2008; Hayes *et al.*, 2010; Filichkin *et al.*, 2011). In Joshua trees, of the 25 251 transcripts that passed minimum expression filters, 64% had significant differential expression between day and night (in a model taking source population into account; 56% of transcripts were significantly different day vs night when taking species into account). While only two transcripts had significant interaction between species and time, many more transcripts (1100) were significantly differentially expressed in both time and species comparisons, suggesting the overall magnitude of expression, rather than the day–night difference, differed between the two species. Transcripts in this latter set included some circadian elements, including *Time for Coffee* (*TIC*) and *Circadian Clock Associated 1* (*CCA1*). Transcriptomic and time course studies between very closely related species within the same genus are largely lacking, and so it remains unclear whether the number of between-species differences in time-of-day responsive genes is notable or not. A study across multiple genera in the Agavoideae highlighted relative conservation of gene families that have variable expression across a 24-h time course, but the extent to which the magnitude or pattern of expression differed between taxa was not fully explored (Heyduk *et al.*, 2022). In general, genes that cycle across time are conserved across plants (Song *et al.*, 2010; McClung, 2013), though there are notable exceptions found in comparisons between CAM and C_3 plants, specifically, where some clock genes have inverse expression patterns in CAM taxa (Yin *et al.*, 2018; Wai *et al.*, 2019). While the genes that were differentially expressed between time and species in Joshua tree do not obviously point to changes strictly associated with CAM, they do suggest species-specific differences in broad-scale carbon and nitrogen metabolism.

Plant carbon and nitrogen metabolism are intrinsically linked through the citric acid cycle and photorespiration. In the latter, photorespiration is responsible for synthesizing amino acids, including serine and glycine, and plants with photorespiratory gene deletions are unable to grow without excess CO_2 (Eisenhut *et al.*, 2019). The citric acid cycle can similarly be a source of substrates for nitrogen assimilation, most notably 2-oxoglutarate (2-OG). Several CAM species have demonstrated increases in citric acid at night, coincident with malate accumulation, but the significance for CAM remains unclear (Lüttge, 1988; Haag-Kerwer *et al.*, 1992; Osmond *et al.*, 1996; Winter & Smith, 2022). While citrate decarboxylation can provide CO_2 to RuBisCO, synthesis of citrate from acetyl-CoA requires CO_2, resulting in no net carbon gain. To date, there is no definitive explanation for the storage of citric acid in CAM plants supported by empirical data. On the other hand, flux-balance modeling in CAM species showed that reversible isocitrate dehydrogenase (IDH) activity could contribute to CO_2 fixation if enough substrate (2-OG) was

present); the reverse activity of IDH provided greater water-use efficiency and did not require an excess of extra energy, thus suggesting the feasibility of an alternate or supplemental CO_2 fixation pathway via IDH (Töpfer *et al.*, 2020). The model further predicted that 2-OG was produced from OAA and glutamate via aspartate aminotransferase (AAT). In this study, we observe increased expression of both *IDH* and *AAT* in eastern Joshua tree (*Y. jaegeriana*) but citrate data do not show accumulation at night, indicating that the altered expression of TCA transcripts in the eastern species (*Y. jaegeriana*) relative to the western (*Y. brevifolia*) is not related to CAM function and instead could simply be due to higher photorespiration rates.

Evolutionary and conservation implications

The presence of CAM in both Joshua tree species has implications for understanding and predicting their responses to ongoing climate change and may inform efforts to protect Joshua tree populations and restore damaged habitats. Accumulating evidence suggests reduced reproduction and survival of Joshua tree seedlings in some populations (Barrows & Murphy-Mariscal, 2012; Sweet *et al.*, 2019; Smith *et al.*, 2023), likely due to increasing temperature extremes and prolonged drought across the Mojave Desert region driven by anthropogenic climate change (Iknayan & Beissinger, 2020; Williams *et al.*, 2020). Species distribution models have repeatedly projected that the trees will lose substantial habitat under projected climate change scenarios (Cole *et al.*, 2011; Barrows & Murphy-Mariscal, 2012; Sweet *et al.*, 2019). At the same time, genetic variation between individuals and physiological plasticity, as shown here, may allow Joshua tree populations to respond to changing climates via adaptive evolution. The potential for evolutionary adaptation could be increased through assisted gene flow (Smith *et al.*, 2023), in which genetic variants associated with CAM activity and resistance to heat stress could be introduced into populations that lack these traits, likely via seed or seedling transfer from populations where those variants are at higher frequency (Aitken & Whitlock, 2013). In addition to providing a basis for assisted gene flow, genetic variation between populations may identify populations harboring adaptive variants for inclusion in protected areas. Conservation biologists have suggested that climate refugia for Joshua trees should be prioritized for protection and managed to reduce the risk of wildfire and other disturbances; genetic variation contained in refugia could be added to the factors prioritized (Barrows & Murphy-Mariscal, 2012; Smith *et al.*, 2023).

Our work also sheds light on the possible origins of the two Joshua tree species. Western (*Yucca brevifolia*) and eastern (*Y. jaegeriana*) species are each exclusively pollinated by separate sister species of brood-pollinating yucca moths. Adaptation to the different pollinators, with subsequent prezygotic isolation, has been the primary focus for studies on the species' divergence (Godsoe *et al.*, 2008; Yoder *et al.*, 2013), especially considering that the two species occupy overlapping, if far from identical, climate regimes (Godsoe *et al.*, 2009; Esque *et al.*, 2023). However, there are also a variety of documented genetic, morphological, and ecological differences between the western (*Y. brevifolia*) and eastern (*Y. jaegeriana*) species, including branching architecture and leaf morphology (Godsoe *et al.*, 2009). Our results document additional genetic differences in citrate metabolism between the two species. Some differences identified here may reflect adaptations to differences in climate regimes by both species. Eastern (*Y. jaegeriana*) *Joshua trees* occur in areas that receive greater summer precipitation and experience higher mean annual temperatures and higher summer maximum temperatures than the western species (*Y. brevifolia*) (Esque *et al.*, 2023). In addition, *Y. jaegeriana*, on average, has a higher moisture deficit, despite higher summer rainfall. Differences in gene expression, particularly in the citric acid cycle and citrate metabolism, may provide benefits to the eastern species (*Y. jaegeriana*) under high temperatures and lower water availability. [Correction added on 17 September 2025, after first online publication: some of the uses of 'eastern' and 'western' in the preceding three sentences have been updated.]

Finally, the presence of CAM in Joshua trees has implications for our broader understanding of CAM evolution within the subfamily Agavoideae. Previous work, based solely on carbon isotope ratios, suggested three independent origins of CAM in the subfamily: one in *Agave sensu lato*, one in the section Yucca of the genus *Yucca*, and one origin in the genus *Hesperaloe* (Heyduk *et al.*, 2016). Placement of Joshua trees within the phylogeny of *Yucca* is uncertain, but the most recent multilocus phylogenies place Joshua trees as sister to the remaining *Yucca* species (Heyduk *et al.*, 2016; Smith *et al.*, 2021). In earlier analyses of ancestral states where Joshua trees were coded as C_3, the single origin of CAM was inferred within *Yucca*; these conclusions need to be reassessed given low-level CAM activity in Joshua tree. Either the ancestor of all *Yuccas* was C_3 + CAM, or CAM has evolved multiple times independently within the genus. Additional sampling of putative C_3 *Yucca* species, along with the use of physiological data in addition to carbon isotopes, can help to better refine the evolutionary history of CAM in *Yucca* and within the Agavoideae more broadly. Additionally, elevated transcript expression at night for a subset of what are considered to be core CAM genes (e.g. PPC and PPCK) but without a correlation to the measured strength of CAM across individuals suggests the control of the CAM phenotype in C3 + CAM species may be more complicated than increasing expression of CAM genes; further work in taxa with intraspecific variation for CAM, like Joshua trees, could be powerful systems with which to interrogate the genomic underpinnings of the upregulation of CAM activity.

Conclusions

In setting out to understand the extent of local adaptation in seedlings of the two Joshua tree species, we found low-level CAM photosynthetic activity in both species, with variation across individuals and populations. However, physiological traits in the different source populations did not correlate with environmental conditions of the home habitat, likely due in part to the temporal mismatch between our single-day physiological measurements and long-term climate data from the home environments. The traits measured are also highly plastic, but such plasticity would require additional common gardens sampled across time to fully

describe. Gene expression comparisons between the two species corroborated CAM presence through the expression of key CAM enzymes, and expression in citric acid cycle and nitrogen metabolism genes were significantly differentially expressed between species. Additional studies could further understanding of the strength of local adaptation vs phenotypic plasticity in Joshua trees. In total, our results reveal metabolic differences between the two species of Joshua tree that have not been described before, and which may have implications for understanding how each species has adapted to Mojave Desert environments, and how each will fare under future changing climatic conditions.

Acknowledgements

The authors would like to thank numerous U.S. Geological Survey employees and interns from the Chicago Botanical Garden who helped establish and maintain the common gardens. Students from Willamette University – Sean Bergan, River McLelland, Emelia Sherman, and Ryan Strobel – assisted with leaf collection for maternal titratable acidity measurements and seed dissection. The authors also thank Dr. Ian Gilman for his helpful comments on the manuscript draft. This work was supported by funding from the National Science Foundation (DEB #2001190/2001180). Any use of trade, firm, or product names is for descriptive purposes only and does not imply endorsement by the U.S. government.

Competing interests

None declared.

Author contributions

KH, LD, TE, CS and JY all contributed to the initial experimental design. KH, SS, BH, MC, BM, JY, DS, CS and TE collected samples and data from the common gardens and/or maternal plants. SS, CK, EM, GY, IS and LH assisted with data processing, including titrations and RNA isolations. MRM annotated the genome and provided the CDS file. MTH conducted isotope analyses. KH led the analysis of the data and writing with input from EM, TE, JY, CS and LD.

ORCID

Lesley A. DeFalco https://orcid.org/0000-0002-7542-9261
Todd C. Esque https://orcid.org/0000-0002-4166-6234
Karolina Heyduk https://orcid.org/0000-0002-1429-6397
Michael T. Hren https://orcid.org/0000-0002-2866-8892
Bryan MacNeill https://orcid.org/0009-0002-5809-046X
Edward V. McAssey https://orcid.org/0000-0003-1568-3361
Michael R. McKain https://orcid.org/0000-0002-9091-306X
Jeremy B. Yoder https://orcid.org/0000-0002-5630-0921

Data Availability

Raw read counts, TPM files, and the CDS sequences used for read mapping are all available on Dryad (DOI: 10.5061/dryad.7pvmcvf3d). Raw RNA-seq reads from both 2021 and 2022 are available through NCBI's Short Read Archive under BioProject PRJNA1132710.

References

Aitken SN, Whitlock MC. 2013. Assisted gene flow to facilitate local adaptation to climate change. *Annual Review of Ecology, Evolution, and Systematics* **44**: 367–388.

Amborella Genome Project. 2013. The Amborella genome and the evolution of flowering plants. *Science* **342**: 1241089.

Archer SR, Predick KI. 2008. Climate change and ecosystems of the Southwestern United States. *Rangelands* **30**: 23–28.

Barrows CW, Murphy-Mariscal ML. 2012. Modeling impacts of climate change on Joshua trees at their southern boundary: how scale impacts predictions. *Biological Conservation* **152**: 29–36.

Beltrán JD, Lasso E, Madriñán S, Virgo A, Winter K. 2013. Juvenile tank-bromeliads lacking tanks: do they engage in CAM photosynthesis? *Photosynthetica* **51**: 55–62.

Bennetzen JL, Schmutz J, Wang H, Percifield R, Hawkins J, Pontaroli AC, Estep M, Feng L, Vaughn JN, Grimwood J *et al.* 2012. Reference genome sequence of the model plant Setaria. *Nature Biotechnology* **30**: 555–561.

Bolger AM, Lohse M, Usadel B. 2014. Trimmomatic: a flexible trimmer for Illumina sequence data. *Bioinformatics* **30**: 2114–2120.

Bray NL, Pimentel H, Melsted P, Pachter L. 2016. Near-optimal probabilistic RNA-seq quantification. *Nature Biotechnology* **34**: 525–527.

Carter PJ, Fewson CA, Nimmo GA, Nimmo HG, Wilkins MB. 1996. Roles of circadian rhythms, light and temperature in the regulation of phosphoenolpyruvate carboxylase in crassulacean acid metabolism. In: Winter K, Smith JAC, eds. *Crassulacean acid metabolism: biochemistry, ecophysiology and evolution*. Berlin, Heidelberg: Springer Berlin Heidelberg, 46–52.

Cheng C-Y, Krishnakumar V, Chan AP, Thibaud-Nissen F, Schobel S, Town CD. 2017. Araport11: a complete reannotation of the *Arabidopsis thaliana* reference genome. *The Plant Journal* **89**: 789–804.

Chollet R, Vidal J, O'Leary MH. 1996. PHOSPHO *ENOL* PYRUVATE CARBOXYLASE: a ubiquitous, highly regulated enzyme in plants. *Annual Review of Plant Physiology and Plant Molecular Biology* **47**: 273–298.

Cole KL, Ironside K, Eischeid J, Garfin G, Duffy PB, Toney C. 2011. Past and ongoing shifts in Joshua tree distribution support future modeled range contraction. *Ecological Applications: A Publication of the Ecological Society of America* **21**: 137–149.

Cole WS, James AS, Smith CI. 2017. First recorded observations of pollination and oviposition behavior in Tegeticula antithetica (Lepidoptera: Prodoxidae) suggest a functional basis for coevolution with Joshua tree (Yucca) hosts. *Annals of the Entomological Society of America* **110**: 390–397.

Covington MF, Maloof JN, Straume M, Kay SA, Harmer SL. 2008. Global transcriptome analysis reveals circadian regulation of key pathways in plant growth and development. *Genome Biology* **9**: R130.

Custer NA. 2017. Ecotype assessment for guiding arid land restoration in the desert southwest of the U.S.

Custer NA, Schwinning S, DeFalco LA, Esque TC. 2022. Local climate adaptations in two ubiquitous Mojave Desert shrub species, *Ambrosia dumosa* and *Larrea tridentata*. *Journal of Ecology* **110**: 1072–1089.

D'Hont A, Denoeud F, Aury J-M, Baurens F-C, Carreel F, Garsmeur O, Noel B, Bocs S, Droc G, Rouard M *et al.* 2012. The banana (*Musa acuminata*) genome and the evolution of monocotyledonous plants. *Nature* **488**: 213–217.

Dole KP, Loik ME, Sloan LC. 2003. The relative importance of climate change and the physiological effects of CO_2 on freezing tolerance for the future distribution of *Yucca brevifolia*. *Global and Planetary Change* **36**: 137–146.

Ebeling SK, Stöcklin J, Hensen I, Auge H. 2011. Multiple common garden experiments suggest lack of local adaptation in an invasive ornamental plant. *Journal of Plant Ecology* **4**: 209–220.

Eisenhut M, Roell M-S, Weber APM. 2019. Mechanistic understanding of photorespiration paves the way to a new green revolution. *New Phytologist* **223**: 1762–1769.

Emms DM, Kelly S. 2019. OrthoFinder: phylogenetic orthology inference for comparative genomics. *Genome Biology* **20**: 238.

Esque TC, Medica PA, Shryock DF, DeFalco LA, Webb RH, Hunter RB. 2015. Direct and indirect effects of environmental variability on growth and survivorship of pre-reproductive Joshua trees, *Yucca brevifolia* Engelm. (Agavaceae). *American Journal of Botany* **102**: 85–91.

Esque TC, Shryock DF, Berry GA, Chen FC, DeFalco LA, Lewicki SM, Cunningham BL, Gaylord EJ, Poage CS, Gantz GE *et al.* 2023. Unprecedented distribution data for Joshua trees (*Yucca brevifolia* and *Y. jaegeriana*) reveal contemporary climate associations of a Mojave Desert icon. *Frontiers in Ecology and Evolution* **11**. doi: 10.3389/fevo.2023.1266892.

Félix-Burruel RE, Larios E, González EJ, Búrquez A. 2024. Population decline of the saguaro cactus throughout its distribution is associated with climate change. *Annals of Botany* **135**: mcae094.

Ferrari RC, Cruz BC, Gastaldi VD, Storl T, Ferrari EC, Boxall SF, Hartwell J, Freschi L. 2020. Exploring C4–CAM plasticity within the *Portulaca oleracea* complex. *Scientific Reports* **10**: 1–14.

Fick SE, Hijmans RJ. 2017. WorldClim 2: new 1-km spatial resolution climate surfaces for global land areas. *International Journal of Climatology* **37**: 4302–4315.

Filichkin SA, Breton G, Priest HD, Dharmawardhana P, Jaiswal P, Fox SE, Michael TP, Chory J, Kay SA, Mockler TC. 2011. Global profiling of rice and poplar transcriptomes highlights key conserved circadian-controlled pathways and *cis*-regulatory modules. *PLoS ONE* **6**: e16907.

Germino MJ, Moser AM, Sands AR. 2019. Adaptive variation, including local adaptation, requires decades to become evident in common gardens. *Ecological Applications: A Publication of the Ecological Society of America* **29**: e01842.

Gilman IS, Edwards EJ. 2020. Crassulacean acid metabolism. *Current Biology: CB* **30**: R57–R62.

Gilman IS, Smith JAC, Holtum JAM, Sage RF, Silvera K, Winter K, Edwards EJ. 2023. The CAM lineages of planet Earth. *Annals of Botany* **132**: 627–654.

Godsoe W, Strand E, Smith CI, Yoder JB, Esque TC, Pellmyr O. 2009. Divergence in an obligate mutualism is not explained by divergent climatic factors. *New Phytologist* **183**: 589–599.

Godsoe W, Yoder JB, Smith CI, Pellmyr O. 2008. Coevolution and divergence in the Joshua tree/yucca moth mutualism. *The American Naturalist* **171**: 816–823.

Goodstein DM, Shu SQ, Howson R, Neupane R, Hayes RD, Fazo J. 2012. Phytozome: a comparative platform for green plant genomics. *Nucleic Acids Research* **40**: D1178–D1186.

Haag-Kerwer A, Franco AC, Luttge U. 1992. The effect of temperature and light on gas exchange and acid accumulation in the C3-CAM Plant *Clusia minor* L. *Journal of Experimental Botany* **43**: 345–352.

Hantson S, Huxman TE, Kimball S, Randerson JT, Goulden ML. 2021. Warming as a driver of vegetation loss in the sonoran desert of California. *Journal of Geophysical Research: Biogeosciences* **126**: e2020JG005942.

Harkess A, Zhou J, Xu C, Bowers JE, Van der Hulst R, Ayyampalayam S, Mercati F, Riccardi P, McKain MR, Kakrana A *et al.* 2017. The asparagus genome sheds light on the origin and evolution of a young Y chromosome. *Nature Communications* **8**: 1279.

Hastings DO, Loik ME. 2025. Summer precipitation pulse response in western Joshua trees (*Yucca brevifolia* Englm.). *Plant Ecology* **226**: 661–672.

Hayes KR, Beatty M, Meng X, Simmons CR, Habben JE, Danilevskaya ON. 2010. Maize global transcriptomics reveals pervasive leaf diurnal rhythms but rhythms in developing ears are largely limited to the core oscillator. *PLoS ONE* **5**: e12887.

Hereford R, Webb RH, Longpré CI. 2006. Precipitation history and ecosystem response to multidecadal precipitation variability in the Mojave Desert region, 1893–2001. *Journal of Arid Environments* **67**: 13–34.

Herppich W, Herppich M, VON Willert DJ. 1992. The irreversible C_3 to CAM shift in well-watered and salt-stressed plants of *Mesembryanthemum crystallinum* is under strict ontogenetic control. *Botanica Acta* **105**: 34–40.

Heyduk K, McAssey EV, Leebens-Mack J. 2022. Differential timing of gene expression and recruitment in independent origins of CAM in the Agavoideae (Asparagaceae). *New Phytologist* **235**: 2111–2126.

Heyduk K, McKain MR, Lalani F, Leebens-Mack J. 2016. Evolution of a CAM anatomy predates the origins of Crassulacean acid metabolism in the Agavoideae (Asparagaceae). *Molecular Phylogenetics and Evolution* **105**: 102–113.

Heyduk K, Moreno-Villena JJ, Gilman IS, Christin P-A, Edwards EJ. 2019. The genetics of convergent evolution: insights from plant photosynthesis. *Nature Reviews. Genetics* **20**: 485–493.

Heyduk K, Ray JN, Leebens-Mack J. 2021. Leaf anatomy is not correlated to CAM function in a C3+CAM hybrid species, *Yucca gloriosa*. *Annals of Botany* **127**: 437–449.

Huxman TE, Hamerlynck EP, Loik ME, Smith SD. 1998. Gas exchange and chlorophyll fluorescence responses of three south-western Yucca species to elevated CO_2 and high temperature. *Plant, Cell & Environment* **21**: 1275–1283.

Iknayan KJ, Beissinger SR. 2020. In transition: Avian biogeographic responses to a century of climate change across desert biomes. *Global Change Biology* **26**: 3268–3284.

International Brachypodium Initiative. 2010. Genome sequencing and analysis of the model grass *Brachypodium distachyon*. *Nature* **463**: 763–768.

Lenz LW. 2007. Reassessment of *Yucca brevifolia* and recognition of *Y. jaegeriana* as a distinct species. *Aliso* **24**: 97–104.

Lepiniec L, Vidal J, Chollet R, Gadal P, Cretin C. 1994. Phosphoenolpyruvate carboxylase: structure, regulation and evolution. *Plant Science* **99**: 111–124.

Loik ME, Huxman TE, Hamerlynck EP, Smith SD. 2000. Low temperature tolerance and cold acclimation for seedlings of three Mojave Desert Yucca species exposed to elevated CO_2. *Journal of Arid Environments* **46**: 43–56.

Lüttge U. 1988. Day-night changes of citric-acid levels in crassulacean acid metabolism: phenomenon and ecophysiological significance. *Plant, Cell & Environment* **11**: 445–451.

McClung CR. 2013. Beyond Arabidopsis: the circadian clock in non-model plant species. *Seminars in Cell & Developmental Biology* **24**: 430–436.

McCormick RF, Truong SK, Sreedasyam A, Jenkins J, Shu S, Sims D, Kennedy M, Amirebrahimi M, Weers BD, McKinley B *et al.* 2018. The *Sorghum bicolor* reference genome: improved assembly, gene annotations, a transcriptome atlas, and signatures of genome organization. *The Plant Journal* **93**: 338–354.

McKain MR, McNeal JR, Kellar PR, Eguiarte LE, Pires JC, Leebens-Mack J. 2016. Timing of rapid diversification and convergent origins of active pollination within Agavoideae (Asparagaceae). *American Journal of Botany* **103**: 1717–1729.

Messerschmid TFE, Wehling J, Bobon N, Kahmen A, Klak C, Los JA, Nelson DB, dos Santos P, de Vos JM, Kadereit G. 2021. Carbon isotope composition of plant photosynthetic tissues reflects a Crassulacean Acid Metabolism (CAM) continuum in the majority of CAM lineages. *Perspectives in Plant Ecology, Evolution and Systematics* **51**: 125619.

Ming R, VanBuren R, Wai CM, Tang H, Schatz MC, Bowers JE, Lyons E, Wang M-L, Chen J, Biggers E *et al.* 2015. The pineapple genome and the evolution of CAM photosynthesis. *Nature Genetics* **47**: 1435–1442.

Munson SM, Webb RH, Belnap J, Andrew Hubbard J, Swann DE, Rutman S. 2012. Forecasting climate change impacts to plant community composition in the S onoran D esert region. *Global Change Biology* **18**: 1083–1095.

Niechayev NA, Mayer JA, Cushman JC. 2023. Developmental dynamics of crassulacean acid metabolism (CAM) in *Opuntia ficus*-indica. *Annals of Botany* **132**: 869–879.

Nobel PS. 1988. *Environmental biology of Agaves and Cacti*. Cambridge, UK: Cambridge University Press.

O'Leary B, Rao SK, Kim J, Plaxton WC. 2009. Bacterial-type phosphoenolpyruvate carboxylase (PEPC) functions as a catalytic and regulatory subunit of the novel class-2 PEPC complex of vascular plants. *The Journal of Biological Chemistry* **284**: 24797–24805.

Osmond CB, Popp M, Robinson SA. 1996. Stoichiometric nightmares: studies of photosynthetic O_2 and CO_2 exchanges in CAM plants. In: Winter K, Smith JAC, eds. *Crassulacean acid metabolism: biochemistry, ecophysiology and evolution*. Berlin, Heidelberg: Springer Berlin Heidelberg, 19–30.

Ouyang S, Zhu W, Hamilton J, Lin H, Campbell M, Childs K, Thibaud-Nissen F, Malek RL, Lee Y, Zheng L *et al.* 2007. The TIGR rice genome annotation resource: improvements and new features. *Nucleic Acids Research* **35**: D883–D887.

Pellmyr O, Segraves KA. 2003. Pollinator divergence within an obligate mutualism: Two yucca moth species (Lepidoptera; Prodoxidae: Tegeticula) on

the Joshua Tree (*Yucca brevifolia*; Agavaceae). *Annals of the Entomological Society of America* **96**: 716–722.

Pellmyr O, Segraves KA, Althoff DM, Balcázar-Lara M, Leebens-Mack J. 2007. The phylogeny of yuccas. *Molecular Phylogenetics and Evolution* **43**: 493–501.

Pimentel H, Bray NL, Puente S, Melsted P, Pachter L. 2017. Differential analysis of RNA-seq incorporating quantification uncertainty. *Nature Methods* **14**: 687–690.

Quezada IM, Zotz G, Gianoli E. 2014. Latitudinal variation in the degree of crassulacean acid metabolism in *Puya chilensis*. *Plant Biology* **16**: 848–852.

R Core Team. 2024. *R: a language and environment for statistical computing*. Vienna, Austria: R Foundation for Statistical Computing. [WWW document] URL https://www.R-project.org/.

Rasmuson KE, Anderson JE, Huntly N. 1994. Coordination of branch orientation and photosynthetic physiology in the joshua tree (*Yucca brevifolia*). *The Great Basin Naturalist* **54**: 204–211.

Reynolds MBJ, DeFalco LA, Esque TC. 2012. Short seed longevity, variable germination conditions, and infrequent establishment events provide a narrow window for *Yucca brevifolia* (Agavaceae) recruitment. *American Journal of Botany* **99**: 1647–1654.

Royer AM, Streisfeld MA, Smith CI. 2016. Population genomics of divergence within an obligate pollination mutualism: selection maintains differences between Joshua tree species. *American Journal of Botany* **103**: 1730–1741.

Scarano F, Duarte H, Rôças G, Barreto S, Amado EF, Reinert F, Wendt T, Mantovani A, Lima H, Barros CF. 2002. Acclimation or stress symptom? An integrated study of intraspecific variation in the clonal plant *Aechmea bromeliifolia*, a widespread CAM tank-bromeliad. *Botanical Journal of the Linnean Society* **140**: 391–401.

Schwinning S, Lortie CJ, Esque TC, DeFalco LA. 2022. What common-garden experiments tell us about climate responses in plants. *Journal of Ecology* **110**: 986–996.

Smith CI, McKain MR, Guimond A, Flatz R. 2021. Genome-scale data resolves the timing of divergence in Joshua trees. *American Journal of Botany* **108**: 647–663.

Smith CI, Pellmyr O, Althoff DM, Balcázar-Lara M, Leebens-Mack J, Segraves KA. 2008. Pattern and timing of diversification in Yucca (Agavaceae): specialized pollination does not escalate rates of diversification. *Proceedings of the Royal Society B: Biological Sciences* **275**: 249–258.

Smith CI, Sweet LC, Yoder J, McKain MR, Heyduk K, Barrows C. 2023. Dust storms ahead: climate change, green energy development and endangered species in the Mojave Desert. *Biological Conservation* **277**: 109819.

Smith SD, Hartsock TL, Nobel PS. 1983. Ecophysiology of *Yucca brevifolia*, an arborescent monocot of the Mojave sesert. *Oecologia* **60**: 10–17.

Smith SD, Monson RK, Anderson JE. 1997. *Physiological ecology of north american desert plants*. Berlin, Heidelberg: Springer.

Song YH, Ito S, Imaizumi T. 2010. Similarities in the circadian clock and photoperiodism in plants. *Current Opinion in Plant Biology* **13**: 594–603.

Starr TN, Gadek KE, Yoder JB, Flatz R, Smith CI. 2013. Asymmetric hybridization and gene flow between Joshua trees (Agavaceae: Yucca) reflect differences in pollinator host specificity. *Molecular Ecology* **22**: 437–449.

Sweet LC, Green T, Heintz JGC, Frakes N, Graver N, Rangitsch JS, Rodgers JE, Heacox S, Barrows CW. 2019. Congruence between future distribution models and empirical data for an iconic species at Joshua Tree National Park. *Ecosphere* **10**: e02763.

Taybi T, Patil S, Chollet R, Cushman JC. 2000. A minimal serine/threonine protein kinase circadianly regulates phosphoenolpyruvate carboxylase activity in crassulacean acid metabolism-induced leaves of the common ice plant. *Plant Physiology* **123**: 1471–1482.

Töpfer N, Braam T, Shameer S, Ratcliffe RG, Sweetlove LJ. 2020. Alternative crassulacean acid metabolism modes provide environment-specific water-saving benefits in a leaf metabolic model. *Plant Cell* **32**: 3689–3705.

Wai CM, Weise SE, Ozersky P, Mockler TC, Michael TP, VanBuren R. 2019. Time of day and network reprogramming during drought induced CAM photosynthesis in *Sedum album*. *PLoS Genetics* **15**: e1008209.

Wickell D, Kuo L-Y, Yang H-P, Dhabalia Ashok A, Irisarri I, Dadras A, de Vries S, de Vries J, Huang Y-M, Li Z *et al.* 2021. Underwater CAM photosynthesis elucidated by Isoetes genome. *Nature Communications* **12**: 6348.

Williams AP, Cook BI, Smerdon JE. 2022. Rapid intensification of the emerging southwestern North American megadrought in 2020–2021. *Nature Climate Change* **12**: 232–234.

Williams AP, Cook ER, Smerdon JE, Cook BI, Abatzoglou JT, Bolles K, Baek SH, Badger AM, Livneh B. 2020. Large contribution from anthropogenic warming to an emerging North American megadrought. *Science* **368**: 314–318.

Winter K. 2019. Ecophysiology of constitutive and facultative CAM photosynthesis. *Journal of Experimental Botany* **70**: 6495–6508.

Winter K, Garcia M, Holtum JAM. 2008. On the nature of facultative and constitutive CAM: environmental and developmental control of CAM expression during early growth of Clusia, Kalanchoë, and Opuntia. *Journal of Experimental Botany* **59**: 1829–1840.

Winter K, Holtum JAM. 2007. Environment or development? Lifetime net CO_2 exchange and control of the expression of Crassulacean acid metabolism in *Mesembryanthemum crystallinum*. *Plant Physiology* **143**: 98–107.

Winter K, Smith JAC. 2022. CAM photosynthesis: the acid test. *New Phytologist* **233**: 599–609.

Yeaton RI, Karban R, Wagner HB. 1980. Morphological growth patterns of Saguaro (*Carnegiea gigantea*: Cactaceae) on flats and slopes in organ pipe cactus National Monument, Arizona. *The Southwestern Naturalist* **25**: 339–349.

Yin H, Guo H-B, Weston DJ, Borland AM, Ranjan P, Abraham PE, Jawdy SS, Wachira J, Tuskan GA, Tschaplinski TJ *et al.* 2018. Diel rewiring and positive selection of ancient plant proteins enabled evolution of CAM photosynthesis in Agave. *BMC Genomics* **19**: 588.

Yoder JB, Smith CI, Rowley DJ, Flatz R, Godsoe W, Drummond C, Pellmyr O. 2013. Effects of gene flow on phenotype matching between two varieties of Joshua tree (*Yucca brevifolia*; Agavaceae) and their pollinators. *Journal of Evolutionary Biology* **26**: 1220–1233.

Zachmann LJ, Wiens JF, Franklin K, Crausbay SD, Landau VA, Munson SM. 2021. Dominant sonoran desert plant species have divergent phenological responses to climate change. *Madrono* **68**: 473–486.

Supporting Information

Additional Supporting Information may be found online in the Supporting Information section at the end of the article.

Fig. S1 Heatmap of z-scaled expression of photorespiratory pathway genes.

Table S1 Tables of 2021 RNA differentially expressed transcript annotations.

Table S2 Physiological data for each individual collected in 2022 used in analyses with outliers/errors removed.

Table S3 Tables of 2022 RNA differentially expressed transcript annotations.

Table S4 Citrate concentrations measured from glasshouse grown plants.

Please note: Wiley is not responsible for the content or functionality of any Supporting Information supplied by the authors. Any queries (other than missing material) should be directed to the *New Phytologist* Central Office.